Preparation and characterization of nanosized $Gd_xBi_{0.95-x}VO_4$:0.05Eu^{3+} solid solution as red phosphor*

Yi Juan(易 娟)[a], Qiu Jian-Bei(邱建备)[a,†], Wang Yu-An(王宇岸)[b], and Zhou Da-Cheng(周大成)[a]

[a] School of Materials Science and Engineering, Kunming University of Science and Technology, Kunming 650093, China
[b] Shenzhen Water (Group) Co. Ltd., Shenzhen 518000, China

(Received 19 January 2014; revised manuscript received 15 March 2014; published online 20 August 2014)

A complete solid solutions with monophasic zircon-type structure of vanadates of formula $Gd_xBi_{0.95-x}VO_4$:0.05Eu^{3+} ($x = 0$–0.95) are synthesized by combined method of co-precipitation and hydrothermal synthesis. Their microstructures and morphologies are characterized by X-ray powder diffraction and transmission electronic microscope, and the results show that each of all the samples has a monophasic zircon-type structure. The absorption spectrum of the prepared phosphor shows a blue-shift of the fundamental absorption band edge with increasing the gadolinium content. Under UV-light and visible-light excitation, all the prepared phosphors show the typical luminescence properties of Eu^{3+} in the zircon-type structure. The emission intensity of $Gd_xBi_{0.95-x}VO_4$:0.05Eu^{3+} ($x = 0.55$) is strongest in all samples under UV-light and visible-light excitations. Finally, the mechanisms of luminescence of Eu^{3+} in the $Gd_xBi_{0.95-x}VO_4$:0.05Eu^{3+} ($x = 0$–0.95) solid solutions are analyzed and discussed.

Keywords: red phosphor, solid solution, monophase, band gap

PACS: 42.70.–a **DOI:** 10.1088/1674-1056/23/10/104224

1. Introduction

White light-emitting diode (W-LED) is one of the most potential candidates for solid-state lighting sources in the lighting industry,[1,2] the present technical bottleneck is that the resulting white light has a poor color rendering index because of color deficiency in the red region.[3] The white LEDs demand red phosphors excited by blue or near ultraviolet (NUV) LED chips.[4,5] However, the red phosphors of sulfides or nitrides suffer poor chemical stability or need rigorous synthesis conditions. Therefore, the search for a stable, inorganic rare-earth-based red phosphor with high absorption in the near-UV/blue spectrum region is an attractive and challenging research task.

Recently, the interest in solid-state materials of vanadium oxide[6,7] doped with rare-earth ion has significantly grown because of their long wavelength properties and excellent chemical stabilities. Among the vanadium oxide, bismuth vanadate ($BiVO_4$) as an important semiconductor material has been extensively studied because it has good ferroelasticity,[8–10] optical property,[11] ionic conductivity,[12] and photocatalytic activity. $BiVO_4$ is known for its three polymorphs: orthorhombic pucherite, tetragonal zircon, and monoclinic clinobisvanite. The lattice constants of zircon-type $BiVO_4$ are $a = 7.2999$ Å, $c = 6.4573$ Å,[13] belonging to the space group $I4_1/amd$. Vandate with zircon structure is considered as good host lattice under near-UV or blue excitation due to its tetrahedron unit. Previous investigations have shown that the Eu^{3+}-doped zircon-type $BiVO_4$ exhibited relatively strong absorption in the near-UV region and red emission with good color purity.[14,15] These results suggest that the Eu^{3+}-doped zircon-type $BiVO_4$ may be a promising candidate as red-emitting phosphor for the LED applications.

Unfortunately, the intensity of red light of these phosphors is weaker than that of the green or blue light of commercial phosphors. Researchers usually attempt to solve the problem of luminous intensity through energy transfer. In this work, we attempt to solve this problem using another strategy, constructing a $BiVO_4$-based solid solution. Compared with other methods, the formation of the $BiVO_4$-based solid solution widens the band gap of $BiVO_4$ and enhance the intensity of emission light.[16,17] Rare-earth (Re) vanadate, $ReVO_4$, has attracted interest as a laser medium and as a host material for rare-earth ions in luminescent displays.[18–21] They also have tetragonal or monoclinic structure at ordinary pressure. In this type of material, $GdVO_4$ has the $ZrSiO_4$ structure ($a = b = 7.2122$ Å and $c = 6.3460$ Å).[22] There are small differences in ionic radius and electronegativity between Gd^{3+} and Bi^{3+}. Due to these reasons, the gadolinium ion could substitute for bismuth in the $BiVO_4$ lattice. While the band gap of $GdVO_4$ lies in the near UV range, the band gap of $BiVO_4$ is located at the edge of the visible range (2.9 eV). Therefore the band gap of the solid solution can be adjusted by changing gadolinium content. Thus, zircon-type $GdVO_4$ is a very ideal candidate material with $BiVO_4$ constructing

*Project supported by the National Basic Research Program of China (Grant No. 2011CB211708), the National Natural Science Foundation of China (Grant Nos. 51272097, 61265004, and 61307111), and the Natural Science Foundation of Yunnan Province, China (Grant No. 2012FD009).

†Corresponding author. E-mail: qiu@kmust.edu.cn

© 2014 Chinese Physical Society and IOP Publishing Ltd

$Gd_xBi_{0.95-x}VO_4$:0.05Eu^{3+} solid solution.

In previous investigations, many different methods have been used to prepare vanadate, but these synthesis methods need high calcination temperature or long synthesis time. Furthermore, the biphase mixture of tetragonal phase and monoclinic phase were obtained using single preparation process. In this work, a new synthesis strategy with low reaction temperature and short synthesis time is addressed, which combines with co-precipitation and hydrothermal methods.[13] And, as far as we know, to date, there has been no report on the fabrication of completed $BiVO_4$-based solid solution with monophasic zircon-type tetragonal by using the traditional synthesis method, nor on the optical properties of such a solution. Based on the progress mentioned above, the purpose of this article is to investigate whether the $Gd_xBi_{0.95-x}VO_4$:0.05Eu^{3+} binary system forms a complete solid solution with the monophase zircon structure. And then, the crystalline structure and the optical properties of $Gd_xBi_{0.95-x}VO_4$:0.05Eu^{3+} solid solution are characterized and analyzed.

2. Experimental details

2.1. Materials

Ammonium vanadate [NH_4VO_3], bismuth nitrate [$Bi(NO_3)_3{\cdot}5H_2O$], europium oxide [Eu_2O_3], gadolinium oxide [Gd_2O_3], ammonia solution [NH_3], and concentrated nitric acid [HNO_3], were all of analytical grade and used without further purification. Distilled water was obtained from laboratory purification system.

2.2. Synthesis of the samples

Europium oxide [Eu_2O_3] and gadolinium oxide [Gd_2O_3] were first converted into the corresponding nitrates by dissolving into concentrated nitric acids respectively. Then the samples were prepared in the following steps: (i) add 12.5 mL of concentrated nitric acid into 50 mL of distilled water and stir the solution; (ii) add 0.01 mol of NH_4VO_3 into the above solution and stir the solution to expedite its dissolution at room temperature; (iii) mix the solutions and stir the mixed solution for 20 min; (iv) add 50 mL of a 0.2-M aqueous solution containing $Bi(NO_3)_3{\cdot}5H_2O$, Gd_2O_3, and $Eu(NO_3)_3$ slowly into the mixed solution; (v) stir the clear, pale lime-yellow solution and adjust the solution pH to pH = 2 with ammonia solution and the solution yields a pale yellow precipitate; (vi) transfer the suspension into a 100-mL teflon-lined stainless steel autoclave, and perform the hydrothermal treatment at 180 °C for 6 h; (vii) take out the reaction suspension, then centrifuge and dry it sequentially. Finally, the powder samples were obtained.

2.3. Characterization

The crystal structure of phosphor samples were characterized by X-ray diffractometer (XRD, Cu-Kα: $\lambda = 1.542$ Å, D8 Advance, German). Transmission electron microscope (TEM) images were taken using a JEOL 2100 transmission electron microscope operating at an acceleration voltage of 200 kV. The optical properties of absorption were measured by ultraviolet-visible diffuse reflectance spectrophotometer (UV-Vis DR, Hitachi U-4100, Japan), and the photoluminescence spectra, including emission and excitation spectra, were obtained using a Hitachi F-7000 spectrophotometer equipped with InGaAs serving as detector with both continuous (150 W, Hitachi F7000, Japan) and pulsed xenon lamps. All the measurements were carried out at room temperature.

3. Results and discussion

3.1. Crystal structure

$BiVO_4$ has a zircon-type structure with space group of $I4_1/amd$, and its lattice parameters are $a = 7.2999$ Å, and $c = 6.4573$ Å, (PDF card No. 014-0133), which are identical with the $GdVO_4$ ($a = 7.2122$ Å, $c = 6.3460$ Å, PDF card No. 086-0996). The XRD patterns of the vanadate-based $Gd_xBi_{0.95-x}Eu_{0.05}VO_4$ ($0 \le x \le 0.95$) phosphors are presented in Fig. 1(a) with different Bi/Gd ratios. The $Gd_xBi_{0.95-x}Eu_{0.05}VO_4$ phosphors are pure in phase and show an excellent match with the tetragonal structure of usual zircon-type of $BiVO_4$ or $GdVO_4$.[23,24] The XRD pattern results preliminary confirm that the crystalline structures of the prepared $Gd_xBi_{0.95-x}Eu_{0.05}VO_4$ ($0 \le x \le 1$) solid-solution samples are completed monophasic zircon-type structures prepared by combining with co-precipitation and hydrothermal methods. With the increase of Gd^{3+} content, and the positions of main diffracted peak of the samples continuously shift toward larger angles, indicating that the lattice parameter decrease with the increase of Gd content. The corresponding lattice parameters are shown in Fig. 1(b). According to Vegard's law, if an element is doped in a crystal lattice, the crystal lattice parameter follows a linear change with the dopant concentration. It is obvious that the lattice parameters of the phosphors decrease gradually with the Gd concentration increasing from 0 to 0.95, which results from the fact that the valence of Gd^{3+} (0.94 Å), Bi^{3+} (1.03 Å), and Eu^{3+} are in steady state that is not easy to gain electrons to form charge defects when Gd^{3+} ion and Eu^{3+} substitute for bismuth. On the other hand, the unit-cell volume of the $GdVO_4$ with Eu^{3+}-doped phosphor is slightly small than that of the $BiVO_4$ itself without exception, which may be ascribed to the fact that the Gd^{3+} and Eu^{3+} ions are expected to occupy the Bi sites in this phosphor since the ionic radii of Eu^{3+} and Gd^{3+} are both slightly smaller than that of Bi^{3+}. Thus, the doping leads to the diminution of lattice volume.

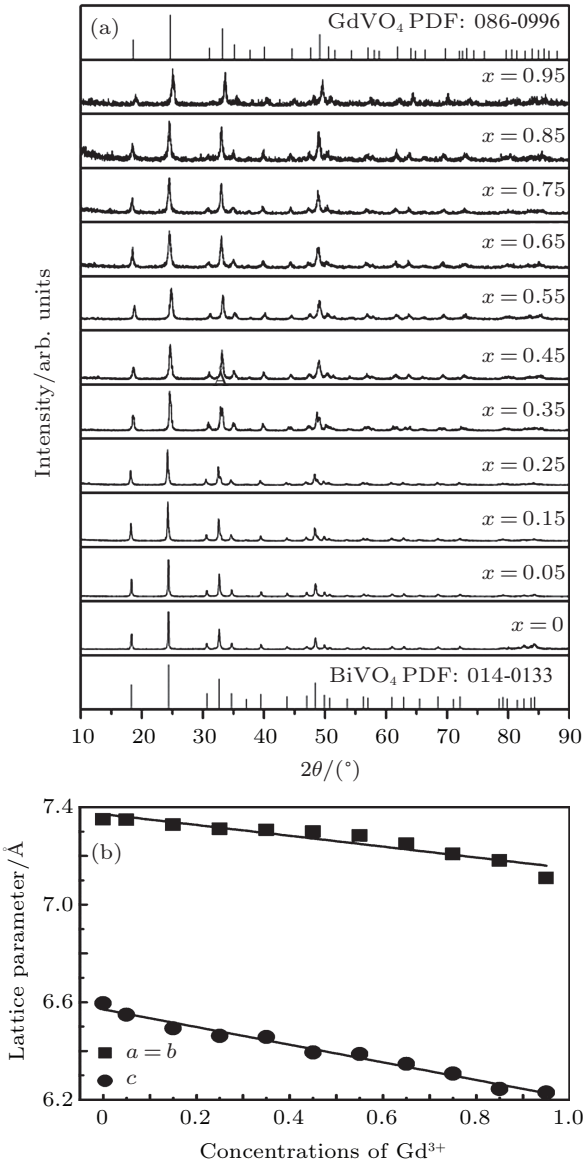


Fig. 1. (a) X-ray diffraction patterns of $Gd_xBi_{0.95-x}VO_4$:0.05Eu^{3+} solid solutions ($0 \le x \le 0.95$), and (b) variations of lattice parameters of $Gd_xBi_{0.95-x}VO_4$:0.05Eu^{3+} solid solutions ($0 \le x \le 0.95$) with Gd^{3+} concentration.

The crystallite size of the $Gd_xBi_{0.95-x}Eu_{0.05}VO_4$ phosphors can be calculated from the broadening of strong XRD peaks, i.e., (2 0 0), (1 1 2), and (3 1 2), by using the Scherrer's equation. The calculated crystallite sizes range from 58 nm to 38 nm. There exists no definite dependence of crystallite size on the Gd content. The morphologies of $Gd_xBi_{0.95-x}Eu_{0.05}VO_4$ ($x = 0.05$, 0.55, and 0.65) are clearly demonstrated by TEM images as shown in Figs. 2(a)–2(c), respectively. The morphology and microstructure of as-prepared $BiVO_4$:Eu^{3+} could be varied by changing the experimental conditions.[14,25] It clearly reveals that they have small nanorod bundles with diameters in a range of 40 nm–60 nm, and are obtained based on co-precipitation, which is in full agreement with those calculated from the XRD patterns. Some researchers claimed that fully crystalline tetragonal bismuth vanadate can be produced by co-precipitation method, so the structure of this sample is a good replication of the zircon-type structure. The high-resolution TEM (HRTEM) images Figs. 2(d)–2(f) show their microstructures, which can also be confirmed by the wide angle XRD results. The spacings of the lattice fringe are all 0.35 nm, which can be attributed to [2 0 0] direction.

For confirming the ratio of elements in the sample, the corresponding energy dispersive X-ray spectroscopy (EDS) spectra are also characterized. From Figs. 2(g)–2(i), these strongest peaks of V, Bi, Gd are clearly indicated together with O, Eu, and Cu peaks. It should be noted that the origin of some strong Cu peaks that appear in the EDS spectra are thought to be from the copper micrometer-grids. No other impurities are observable in the images, implying that the resulting phosphors are pure in chemical composition. In the cases of $Gd_xBi_{0.95-x}VO_4$:0.05Eu^{3+} ($x = 0.05$, 0.55, 0.65), in the upper-right corners of Figs. 2(g)–2(f) there are shown the relative atomic percentages of Bi, Gd, and Eu, which accord well with the stoichiometric ratios in the precursors. Inside the crystallites, all of the elements are distributed well. In short, the presence of the signals of elements V, O, Eu, Bi, and Gd demonstrates that the Eu and Gd elements have been successfully doped into the host.

3.2. Optical absorption

Figure 3 shows the results of the UV-vis absorption spectra of $Gd_xBi_{0.95-x}Eu_{0.05}VO_4$ ($0 \le x \le 0.95$) solid-solution with different gadolinium content values. For all samples, the fundamental light absorption is dominantly ascribed to electron transfer from the valence band to the conduction band. One main contribution of the absorption spectra on the $Gd_xBi_{0.95-x}Eu_{0.05}VO_4$ ($0 \le x \le 0.95$) systems can be analyzed. From band structure calculations, it appears that the gap of gadolinium vanadate mostly consists of a charge transfer between O_{2p} non-bonding levels of the valence band and V_{3d} levels of the conduction band. Upon replacing Gd^{3+} with Bi^{3+} the basic features of the $GdVO_4$ electronic structure are retained, but additional bands arise which can be attributed to the Bi_{6s} and Bi_{6p} orbitals.[26] When Gd^{3+} is substituted for Bi^{3+}, the full Bi_{6s2} levels shift toward higher energy because of the interaction of charges with the full O_{2p} levels, while the empty Bi_{6p} levels are shifted toward lower energy through hybridization with the empty V_{3d} levels. The absorption edges of pure $GdVO_4$ and $BiVO_4$ are at about 400 nm and 435 nm (the band gap energies of tetragonal structures of $BiVO_4$ and $GdVO_4$ have been reported to be 2.9 eV and 3.1 eV) respectively. In other words, the formation of the solid solution widens the band gap of $BiVO_4$, which can be reasonably understood, when considering the larger band gap of $GdVO_4$. The absorption band undergoes a blue shift with the increase of Gd^{3+} ions concentration. The absorption edges of various

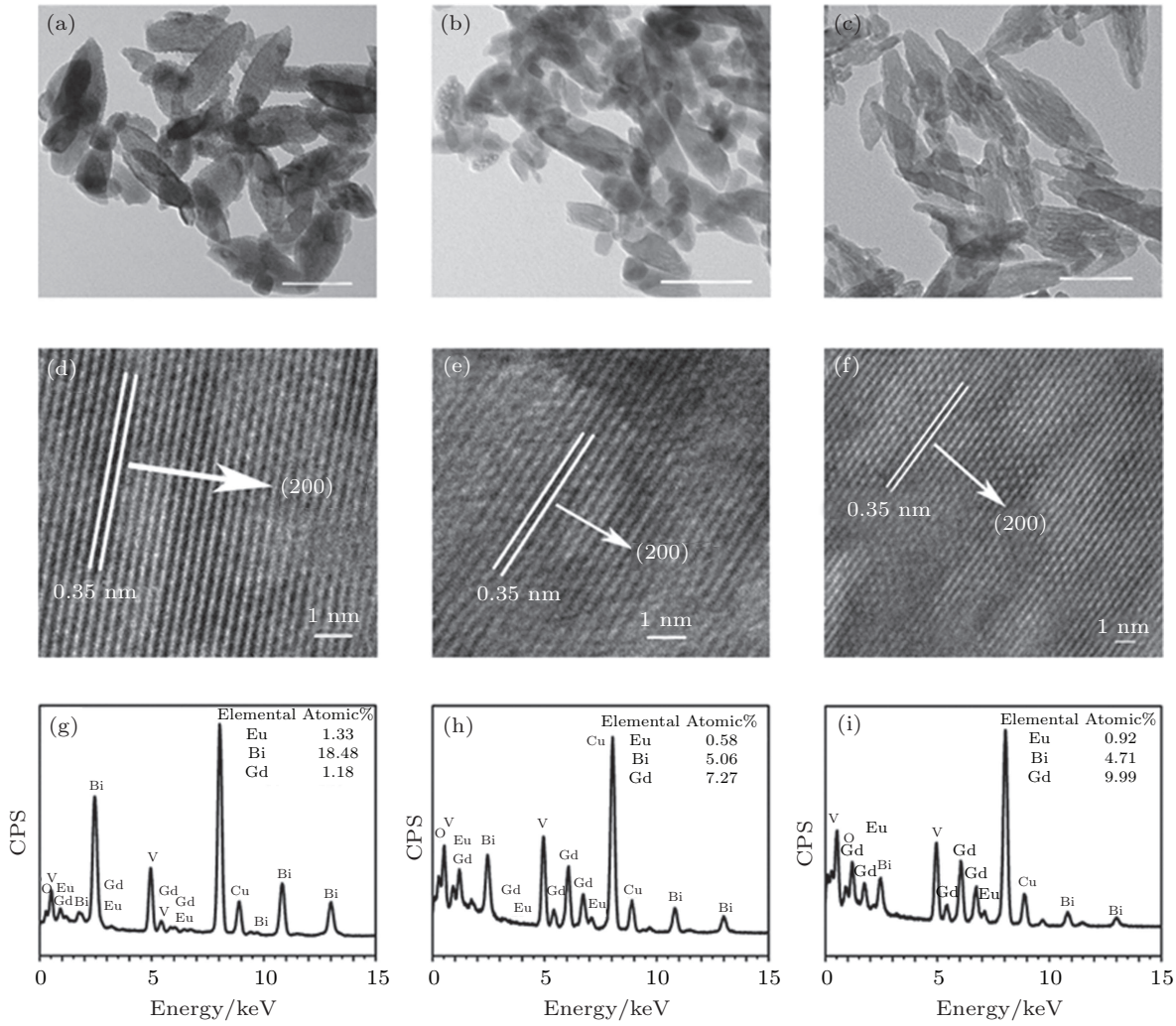


Fig. 2. (a)–(c) Transmission electron microscopic images of $Gd_xBi_{0.95-x}VO_4$:0.05Eu^{3+}, (d)–(f) the high-resolution TEM images, and (g)–(i) EDX spectra ($x = 0.05$, 0.55, 0.65).

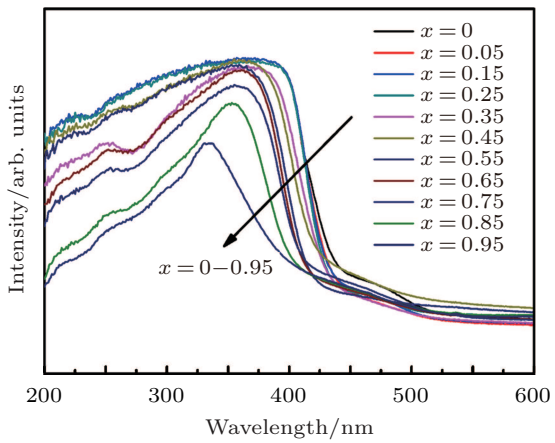


Fig. 3. (color online) The UV-Vis absorption spectra of $Gd_xBi_{0.95-x}VO_4$:0.05Eu^{3+} ($x = 0 \sim 0.95$) solid-solution.

$Gd_xBi_{0.95-x}Eu_{0.05}VO_4$ ($0 \leq x \leq 0.95$) solid solution depends on the ratio of Bi to Gd, hence, it is located on the edge of $BiVO_4$ (400 nm) to $GdVO_4$ (435 nm). The band gap of solid solution changes into the form of a continuous parabola with the variation of its solid solubility, thus causing successive blue shift on the absorption edge. To the best of our knowledge, the physical properties of continuous solid solution change continuously with composition. According to this principle, the change of composition could be determined by the research on the band gap. Finally, the formulation of continuous solid solution could be determined. Each of the synthesized samples exhibit a pale yellow color (the tetragonal structure of $BiVO_4$ is in pale yellow color). This implies that the band gap of $Gd_xBi_{0.95-x}Eu_{0.05}VO_4$ ($0 \leq x \leq 0.95$) solid-solution could be adjusted and controlled by changing the value of x, all of the samples are of tetragonal structure, which is their most important feature.

3.3. Luminescence properties

Figure 4 shows the emission spectra of the samples with different gadolinium content values, excited by 325-nm wavelength. These distinct emission bands are narrow and attributed to the f–f transition of Eu^{3+}, we can identify their origins as follows: $^5D_0 \rightarrow {}^7F_2$ (619 nm), $^5D_0 \rightarrow {}^7F_1$ (594 nm), $^5D_0 \rightarrow {}^7F_3$ (652 nm), $^5D_0 \rightarrow {}^7F_4$ (703 nm). From Fig. 4, it is obvious that the splitting of $^5D_0 \rightarrow {}^7F_2$ transition is observed. This suggests that the Eu^{3+} ions are located

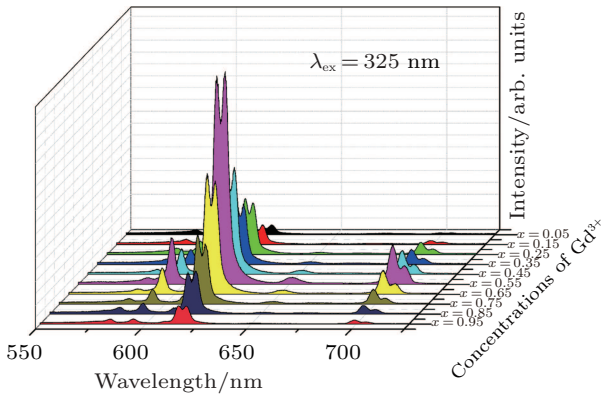


Fig. 4. (color online) The room temperature emission spectra of $Gd_xBi_{0.95-x}VO_4$:0.05Eu^{3+} ($x = 0.05 \sim 0.95$) solid-solution excited by near UV-light ($\lambda_{ex} = 325$ nm).

in a strong crystal field. With increasing the Gd^{3+} ion concentration, the emission lines are all enhanced significantly, this increase seems to be monotonic only when more than half of the Bi^{3+} ions are substituted by gadolinium ions. For substitutions exceeding $x = 0.55$, the luminescence intensity decreases. Theoretically, if the ions are separated far from each other, the energy transfer is not efficient. On the other hand, the closely spaced ions will lead to deleterious cross-relaxation, which reduces the emission efficiency.[27] Thus, the fluorescence emission of the solid-solution sample is affected by the distance between emission centers (Eu^{3+}) and VO_4^{3-}. The Gd^{3+} ions are carefully chosen to have an ionic size slightly smaller than Bi^{3+} to make the replacement of Bi^{3+} with the ions possible. The purpose of Gd^{3+} ions doping is to slightly change the volume of the unit-cell in the crystal and then improve the energy transfer efficiency to Eu^{3+} ions, and eventually increase the fluorescence emission. Thus, the fluorescence emission could be adjusted by Gd^{3+} ions doping. When a small number of Gd^{3+} ions are doped, they may occupy the lattice sites. It is well known that small size ions are doped, they will possibly occupy the substitution or interstitial positions. The crystal unit-cell will diminish when only occupying the lattice sites.[28] Then comparing the XRD pattern in Fig. 1(a) with standard PDF card 014-0133, it is found that all the diffraction peaks slightly shift toward large diffraction angles, suggesting that the volume of unit cell shrinks after the Gd^{3+} ion doping. The PL intensity increasing up to $x = 0.55$ may be caused by the fact that the solid-solution with proper crystal unit cell efficiently absorbs the excitation energy and transfers it to the Eu^{3+} activator. As Gd^{3+} ions substitute for Bi^{3+} ions in $BiVO_4$ lattice, the fluorescence emission of the solid-solution is expected to rise. When the number of Gd^{3+} ions is further increased, the decrease in emission intensity may be due to the extreme shrinking of unit-cell, which causes the emission centers (Eu^{3+}) and VO_4^{3-} to become closer. Thus, the quenching might occur. We believe that the quenching is caused by energy transfer among activators, that is, energy transfer occurs from one activator to another until an energy sink in the lattice is reached.[27] Thus, energy transfer should be very sensitive to concentration. Besides, the shrinkage of the unit-cell causes more surface defects, which might be caused by the electron cloud of the ions which is distorted due to the imbalance of the crystal lattice, increased surface area and more broken bonds that appear on the surface of the unit-cell after substituting a relatively large number of Gd^{3+} ions. Therefore, the mixing of Gd/Bi ration can tune the emission spectrum intensity, and account for the excellent red luminescence.

For Eu^{3+}-doped samples, the excitation spectra monitored at 619 nm are shown in Fig. 5(a), which recorded and composed of two main parts. One is a broad excitation peak in the range of 220 nm–420 nm with a prominent bands locating at 325 nm. It can be ascribed to the $^1A_1$–$^1T_1$ transition of VO_4^{3-}. In fact, this broad excitation peak is overlapped with the charge transfer of Eu^{3+}-doped lanthanide compounds with the increase of Gd concentration. The representative one ($x = 0.25$) is shown in Fig. 5(b), it can be well fitted and decomposed into two curves. Evidently, band 1 is corresponding to the $^1A_1$–$^1T_1$ transition of VO_4^{3-}; band 2 is corresponding to the CT of Eu^{3+}-doped $GdVO_4$–$BiVO_4$ solid-solution that locating at 275 nm. Another part is from 400 nm

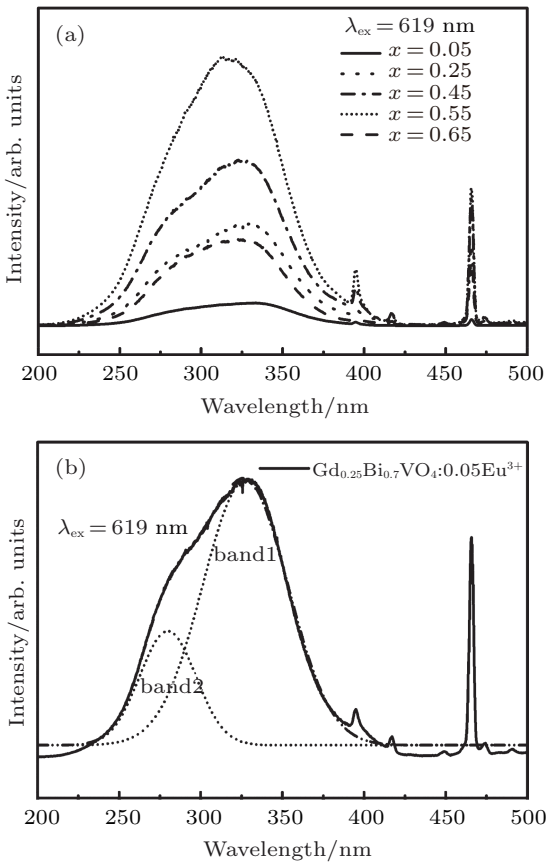


Fig. 5. The panel (a) shows the room temperature excitation spectra of $Gd_xBi_{0.95-x}VO_4$:0.05Eu^{3+} solid-solution by monitoring the $^5D_0 \rightarrow {}^7F_2$ transition of Eu^{3+} ions ($\lambda_{em} = 619$ nm). (b) Excitation spectrum of sample $x = 0.25$ ($\lambda_{em} = 619$ nm) in the range of 220 nm–420 nm. Solid line (black) is measured curve and another (dash) is fitting curve; short dot lines are two synthesized Lorentzian curves.

to 500 nm with several sharp peaks. The peaks at 384 nm, 393 nm, 418 nm, and 466 nm ascribed to the transitions of Eu^{3+}: $^7F_0 \rightarrow {}^5G_{2-4}$, $^7F_0 \rightarrow {}^5L_6$, $^7F_0 \rightarrow {}^5D_3$, $^7F_0 \rightarrow {}^5D_2$ respectively. In the case of $Gd_xBi_{0.95-x}Eu_{0.05}VO_4$ the band edge shifts to short wavelength with increasing Gd^{3+} ions concentration. The band edge in the excitation spectrum moves from 325 nm to 275 nm. This shift occurs because the band gap could be adjusted accused to extra absorption involving the VO_4^{3-} component in addition to the CT bands. In addition, among excitation lines, the intensity of the Eu^{3+} line at 466-nm excitation peaks is much stronger than the others. This suggests that the intrinsic transition in Eu^{3+} ion levels is more efficient for the energy migration to europium ions in the solid-solution phosphors, indicating that the solid-solution phosphors could enhance the blue LED chip excitation in obtaining the characteristic red emissions. These results indicate that $Gd_xBi_{0.95-x}Eu_{0.05}VO_4$ could be excited by near UV light and visible light, resulting in realizing suitable for different LED chips.

As shown in Fig. 5(b), band 2 is considered as the CT of Eu^{3+}-doped $GdVO_4$–$BiVO_4$ solid-solution. This point is fully in agreement with the behavior of a wide variety of charge transfer (CT) in Eu^{3+}-doped lanthanide compounds.[29,30] In the previous work, the relationship between the experimental charge transfer energy of Eu^{3+} and the corresponding average energy gap E_g has been studied. It allows us to predict the CT position of Eu^{3+}-doped lanthanide compounds with knowledge of the crystal structure and index of refraction. In this model, the CT position of Eu^{3+}-doped $GdVO_4$–$BiVO_4$ solid-solution can be analyzed. Samples are well fitted with equation as follows:

$$\overline{E_g} = \frac{\sum_v (N^v \times E_g^v)}{\sum_v N^v}, \tag{1}$$

where N^v denotes the coordination number of v bond and E_g^v is its average energy gap.

The calculated results are compiled in Table 1. The refractive indexes n are listed in column 2. The β values are listed in column 3. The bond types between the ligands and the center ions substituted by Eu^{3+} are shown in column 4. The relevant weighted means of average energy gap for the type Eu–X bond is listed in column 5. The experimental CT energies are shown in column 6. From the calculated chemical bond parameters in Table 1, we plot the experimental CT energies in $Gd_xBi_{0.95-x}Eu_{0.05}VO_4$ samples (in column 6) against the corresponding average energy gap E_g (in column 5). The relationship between them is shown in Fig. 1. The expression between them can be written as

$$E_{CT} = 2.542 + 0.171 \times \overline{E_g}. \tag{2}$$

From Table 1, it can be found that the $E_{CT,calcd}$ is suitable for excellent $E_{CT,exptl}$, indicating that the band 2 in Fig. 5(b) is the CT of Eu^{3+}.

Table 1. Crystal data and calculated bond parameters for crystals in Eu^{3+}-doped $GdVO_4$–$BiVO_4$ solid-solution.

Crystal	n	β	Bond type	E_g^μ	$E_{CT,exptl}$	$E_{CT,calcd}$
$GdVO_4$	2.1139	0.088	Gd-O	11.444	4.51	4.48

It is well known that vanadium oxide doped with rare-earth ion is a typical host sensitizing luminescence material. Its emission intensity and efficiency mainly depend on the host absorption and energy transfer from the host to activators. The possible energy transfer processes are shown in Fig. 6. As shown in Fig. 6 ($x = 0$), under the excitation at 325 nm, the electron of the $BiVO_4$:Eu^{3+}crystal absorbs energy and transits from the highest valence band to the conduction band. The Eu^{3+} ions first populate the lower $^5D_0$ level from the upper $^5D_2$ level via non-radiative transition, then return to the ground state with diverse probabilities and radiate the $^5D_0 \rightarrow {}^7F_J$ emission. Instead of transferring energy to Eu^{3+}, the energy may be relaxed to the ground state of the VO_4^{3-}group directly. But the relaxation process is less efficient than the transition process in this case; the emission peak of VO_4^{3-} is hard to find. However, for the $Gd_{0.55}Bi_{0.4}Eu_{0.05}VO_4$, when being excited at 325 nm, the lowest of the conduction band is matching in the $^5D_3$ level of Eu^{3+}, the intrinsic 4f–4f emission of Eu^{3+} is very intense. It indicates that the observed intense red light emission in Fig. 4 is very likely due to the high-efficient energy transfer from the host to Eu^{3+}. The solid solution achieves the purpose that the band gap could be adjusted and controlled by changing the value of x, then tuning the emission spectra intensity, thereby accounting for the excellent red luminescence.

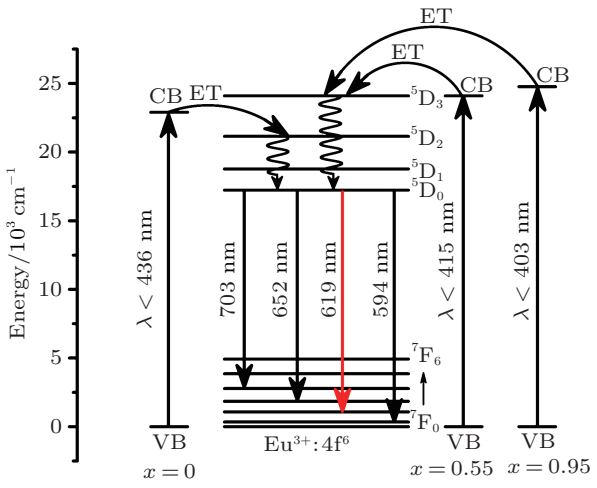


Fig. 6. (color online) Schematic diagrams of energy levels of Eu^{3+} ion in $Gd_xBi_{0.95-x}VO_4$:0.05Eu^{3+} crystal as well as possible energy transfer processes.

4. Conclusions

A monophasic zircon-type $Gd_xBi_{0.95-x}Eu_{0.05}VO_4$ ($0 < x < 1$) solid-solution is successfully synthesized by combining with co-precipitation and hydrothermal method. Through the introduction of the material ($GdVO_4$) that has the same crystalline structure as zircon-type $BiVO_4$, the solid solution is formed. Based on the results of UV-Vis absorption characterization, it is found that the band gap of $Gd_xBi_{0.95-x}Eu_{0.05}VO_4$ could be adjusted with gadolinium content. This phosphor achieves the purpose that the red light of the phosphors has high luminescent efficiency and can be excited efficiently in near UV region and visible light at 466 nm. Especially, the emission intensity of $Gd_xBi_{0.95-x}Eu_{0.05}VO_4$ ($x = 0.55$) is the strongest in emission intensities of all samples. These results can inspire the future development of the red phosphor that can be excited by different LED chips.

References

[1] Zhou T L, Song Z, Song X P, Bian L and Liu Q L 2010 *Chin. Phys. B* **19** 127808

[2] Jiang T M, Yu X, Xu X H, Zhou D C, Yu H L, Yang P H and Qiu J B 2014 *Chin. Phys. B* **23** 028505

[3] Li P L, Wang Y S, Zhao S L, Zhang F J and Xu Z 2012 *Chin. Phys. B* **21** 127804

[4] Nersisyan H, Won H I and Won C W 2011 *Chem. Commun.* **47** 11897

[5] Zhang Q T, Zhang L, Han P D, Chen Y, Yang H and Wang L X 2011 *Prog. Chem.* **23** 1108

[6] Neeraj S, Kijima N and Cheetham J A K 2004 *Solid State Commun.* **131** 65

[7] Zhang Q, Guo C, Shi C and Lü S Z 2000 *J. Alloys Compd.* **309** 10

[8] Bierlein J D and Sleight A W 1975 *Solid State Commun.* **16** 69

[9] Manolikas C and Amelinckx S 1980 *Phys. Status Solidi A* **60** 167

[10] David W I F 1983 *J. Phys. C: Solid State Phys.* **16** 5093

[11] Ren L, Jin L, Wang J B, Yang F, Qiu M Q and Yu Y 2009 *Nanotechnology* **20** 15603

[12] Hirota K, Komatsu G, Yamashita M, Takemura H and Yamaguchi O 1992 *Mater. Res. Bull.* **27** 823

[13] Bhattacharya A K, Mallick K K and Hartridge A 1997 *Mater. Lett.* **30** 7

[14] Wang Q M, Li Y, Zeng Z and Pang S T 2012 *J. Nanopart. Res.* **14** 1076

[15] Zheng Y H, Tan J J, Huang L X, Tan D H, Li Y, Lin X X, Huo S M, Lin J T and Wang Q M 2013 *Mater. Lett.* **113** 90

[16] Neeraj S, Kijima N and Cheetham A K 2004 *Chem. Phys. Lett.* **387** 2

[17] Kazuhiko Maeda and Kazunari Domen 2014 *J. Catal.* **310** 67

[18] Tian L and Mho S 2007 *J. Lumin.* **122** 99

[19] Sohn K S, ZeonW, Chang H, Lee S K and Park H D 2002 *Chem. Mater.* **14** 2140

[20] Chen L, Chen K J, Hu S F and Liu R S 2011 *J. Mater. Chem.* **21** 3677

[21] Luo Q, Shen S, Lu G, Xiao X, Mao D and Wang Y 2012 *RSC Advances* **2** 616

[22] Fuess H and Kallel A 1972 *J. Solid State Chem.* **5** 11

[23] Bhattacharya A K, Mallick K K and Hartridge A 1997 *Mater. Lett.* **30** 7

[24] Mullica D F, Sappenfield E L, Abraham M M, Chakoumakos B C and Boatner L A 1996 *Inorganica Chimica Acta* **248** 85

[25] Mahalley B N, Dhoble S J, Pode R B and Alexander G 2000 *Appl. Phys. A* **70** 39

[26] Dolgos M R, Paraskos A M, Stoltzfus M W, Yarnell S C and Woodward P M 2009 *J. Solid State Chem.* **182** 1964

[27] Blasse G 1968 *Phys. Lett. A* **28** 444

[28] Dou Q Q and Zhang Y 2011 *ACS Publications* **27** 13236

[29] Vandervort D and Blasse G 1991 *Chem. Mater.* **3** 1041

[30] Li L, Zhou S H and Zhang S Y 2007 *J. Phys. Chem. C* **111** 3205